Profile Measurements of Micro-aspheric Surfaces Using an Air-bearing Stylus with a Microprobe

Atsushi Shibuya[1,#], **Wei Gao**[1], **Yasuo Yoshikawa**[1], **Bing-Feng Ju**[1] and **Satoshi Kiyono**[1]

1 Dept. of Nanomechanics, School of Engineering, Tohoku University, Japan
Corresponding Author / E-mail: shibuya@nano.mech.tohoku.ac.jp, TEL: +81-22-795-6953, FAX: +81-22-795-6953

A novel scanning probe measurement system was developed to enable precise profile measurements of micro-aspheric surfaces. An air-bearing stylus with a microprobe was used to perform the surface profile scanning. The new system worked in a contact mode and had the capability of measuring micro-aspheric surfaces with large tilt angles and complex profiles. Due to limitations resulting from the contact mode, such as possible damage caused by the contact force and lateral resolution restrictions from the curvature of the probe tip, several system improvements were implemented. An air bearing was used to suspend the shaft of the probe to reduce the contact force, enabling fine adjustments of the contact force by changing the air pressure. The movement of the shaft was measured by a linear encoder with a scale attached to the actual shaft to avoid Abbe errors. A 50-μm-diameter glass sphere was bonded to the tip of the probe to improve the lateral resolution of the system. The maximum contact force of the probe was 10 mN. The shaft was capable of holding the probe continuously if the contact force was less than 40 mN, and the resolution of the probe could be as high as 10 nm. The performance of the new scanning probe measurement system was verified by experimental data.

NOMENCLATURE

e_{CP} = positioning error along the X-axis of the linear stage
e_{CT} = horizontal straightness error of the linear stage
e_{CY} = yawing error of the linear stage
e_{SP} = radial motion along the X-axis of the spindle
e_{ST} = axial motion of the spindle
e_{SY} = tilt motion around the Y-axis of the spindle

1. Introduction

Micro-aspheric lenses are important components that are widely used in medical endoscopes and fiber-optic communication systems.[1] To guarantee the performance of such systems, the required profile accuracy of micro-aspheric lenses is usually within 100 nm.[2] However, no commercial facilities are presently available that can provide such high-accuracy profile measurements. It is therefore impossible to obtain an online assessment of the machining accuracy and evaluate the machining error.

In this study, we developed a new scanning probe measurement system in which an air-bearing stylus with a microprobe was used for surface profile scanning. The new system operated in a contact-mode and had the capability of measuring micro-aspheric surfaces with large tilt angles and complex profiles. To reduce the contact force, an air bearing was used to suspend the shaft of the probe.[3] The movement of the shaft was measured by a linear encoder with a scale attached to the actual shaft to avoid Abbe errors. A 50-μm-diameter glass sphere was bonded to the tip of the probe to improve the lateral resolution of the system. The sphere facilitated a high degree of accuracy and it introduced a nondestructive test capability. The target accuracy of the new scanning probe measurement system was ±10 nm, which was achieved, as demonstrated by experimental data.

2. Outline of the contact-mode displacement sensor

Figure 1 shows a schematic diagram of the air bearing and its assembled relationship with the contact-mode probe. Three air inlets were predefined in the ektexine of the cylinder that were capable of suspending the shaft, feeding the shaft forward, and withdrawing the shaft backward. Adjustments to the air pressure could also change the contact force between the probe and sample surface. The movement of the shaft was measured by the linear encoder. Figure 2 gives a full-scale photograph of the contact-mode profile measurement system.

The specifications of the contact-mode displacement sensor are listed in Table 1. The linear encoder had two outputs of symmetric 90° phase-shifted sinusoidal signals that were loaded in a counter board. After interpolation, the encoder could achieve a resolution of 0.5 nm.[4]
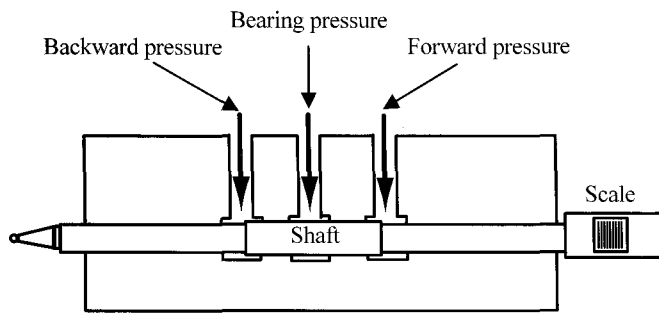
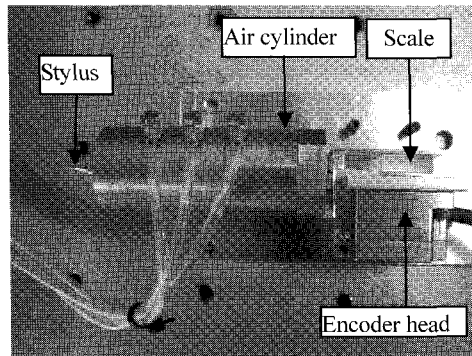Fig. 1 Contact-mode displacement sensor probe

Fig. 2 Photograph of the contact-mode displacement sensor probe

Table 1 Specifications of the contact-mode displacement sensor

Manufacturer	Linear encoder	Heidenhain
	Probe	Toshiba
Grating period	4 μm	
Signal period	2 μm	
Interpolation no.	4096	
Resolution	0.49 nm	
Shaft length	69.5 mm	
Measurement range	1.7 mm	
Output format	Two signals (A phase, B phase)	

3. Experiment

3.1 Stability of the displacement sensor

The air supply for the air bearing was well controlled through a precision regulator and maintained relatively constant so that a given air pressure could be obtained to within 3 kPa for 10 min. Thus the pressure variation was within 3% of the set value, which was at least 0.1 MPa.

The stability of the system for different air-bearing pressures was measured, as shown in Fig. 3. The probe shaft was pressed against the sample surface and then kept stationary for 300 s. The output of the displacement senor was recorded continuously during the process. The forward and backward pressures were maintained constant, but the bearing pressure was set to 0.10, 0.20, or 0.30 MPa. The figure shows that the output value had no direct relation to the air-bearing pressure. Although higher air-bearing pressures could lead to greater output drifts, we observed little effect from this drift over short periods of time. This drift can therefore be ignored in micro-aspheric surface measurements since the entire measuring time is typically about 10 s.

3.2 Contact force of the displacement sensor

A photograph of the experimental setup for the contact force evaluation is shown in Fig. 4. A strain gauge was employed; its specifications are listed in Table 2. The compressed air pressures for
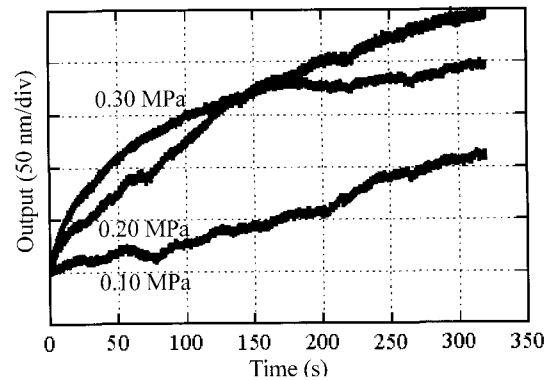

Fig. 3 Stability of the displacement sensor at various air pressures

the different inlets were carefully adjusted to achieve the smallest possible contact force. The resulting values can be found in Table 3. The displacement sensor probe was mounted on a manual stage and driven forward to contact with the strain gauge probe. The contact force measurements were taken at this point. A gradual displacement was applied to the probe shaft by the manual stage until the shaft reached its ultimate measurement range. The measured contact force is shown in Fig. 5; its value was less than 10 mN over the entire measurement range.

Table 2 Specifications of the strain gauge

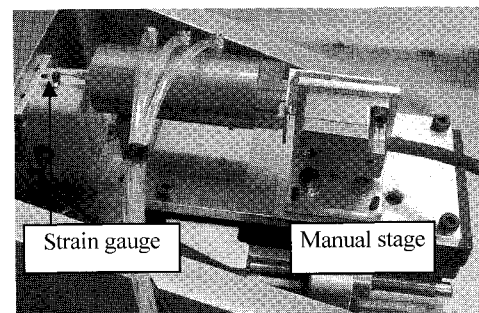| Manufacturer	Kyowa Electric Instruments Co.
Rated output	1753 μV/V
Nonlinearity	±0.5% R.O.
Rated capacity	49.03 mN
Hysteresis	±0.5% R.O.

Fig. 4 Photograph of the experimental setup used to measure the contact force

Table 3 Experimental conditions used for the contact force measurements

Measurement range	1.7 mm
Bearing pressure	0.206 MPa
Forward pressure	0.131 Mpa
Backward pressure	0.087 MPa

3.3 Resolution of the displacement sensor

The system shown in Fig. 6 was developed to evaluate the resolution of the displacement sensor. A linear stage was used to provide discrete 10-nm step movements after the sensor probe and linear stage were in firm contact with each other. The corresponding reactive motion of the displacement sensor was output and recorded continuously.

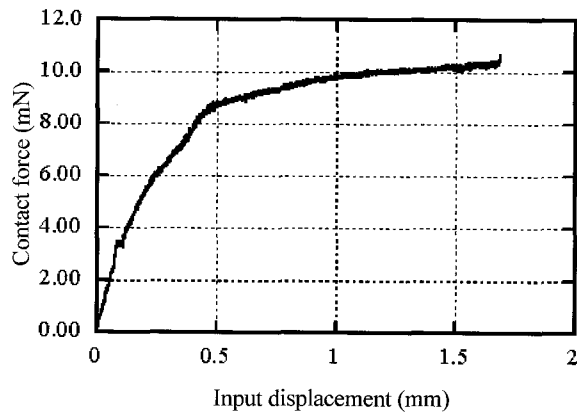The linear stage ran in a closed-loop mode in which the output

Fig. 5 Contact force of the contact-mode displacement sensor

Fig. 7 Resolution of the displacement sensor

position of the linear encoder served as the feedback signal. The specifications of the linear stage are given in Table 4.

Then sampled output of the displacement sensor was 500 points per step. The experimental results, shown in Fig. 7, indicate that the output of the displacement probe kept pace with the linear stage movements. The resolution of this displacement sensor could therefore be defined as 10 nm.
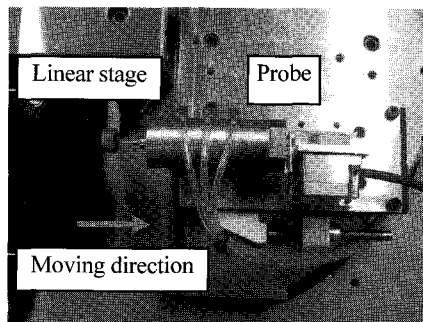

Fig. 6 Experimental setup used to evaluate the resolution of the displacement sensor

Table 4 Specifications of the linear stage

Manufacturer	NTN Co.
Drive system	Linear motor
Bearing	Aerostatic bearing
Stroke	300 mm
Linear encoder resolution	0.28 nm
Stopping accuracy	5 nm

3.4 Linearity of the displacement sensor

A laser interferometer, with specifications given in Table 5, was used to check the linearity of the displacement sensor. The experimental setup is shown in Fig. 8. The laser interferometer and displacement probe were arranged in a single straight line. A special target with a well polished surface was mounted on the linear stage. The target was firmly in contact with the displacement sensor, and the well polished surface was attached to its backside to reflect the laser beam. The target was driven by the linear stage. The same movement distances were generated for both the laser interferometer and displacement sensor, but in opposite directions. The outputs of the interferometer and displacement sensor were recorded simultaneously and the moving signal of the linear stage was used as a reference. The moving speed of the linear stage was 0.08 mm/s and the sampling interval was 2 µm.

The stability of the laser interferometer and the linearity error of the displacement sensor are shown in Figs. 9 and 10, respectively.
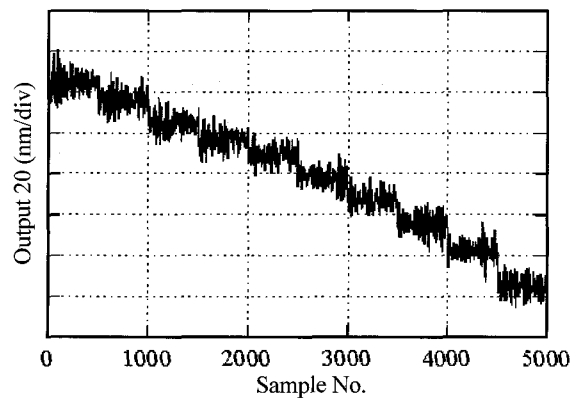
The vertical axis of Fig. 10 gives the output difference between the displacement probe and the laser interferometer, while the horizontal axis shows the output of the laser interferometer. The linearity error of the displacement sensor was approximately 0.005% of the full measurement range. The two figures show that the linearity error of the displacement sensor within the entire measurement range was comparable to the stability of the laser interferometer system.

An incontestable axial alignment error between the interferometer and displacement probe produced a cosine error. As shown in Fig. 11, if the alignment error was less than 0.2°, the cosine error was less than 10 nm over the entire measurement range of 1.7 mm.

Table 5 Specifications of the laser interferometer system

Manufacturer	Hewlett Packard
Laser system	He–Ne gas laser
Wavelength	632.991 nm
Resolution	2.5 nm (4-path interferometer)

3.5 Bonding a micro-sphere to the stylus

To improve the lateral resolution, glass spheres with different diameters were bonded to the tip of the stylus.[5] A homemade apparatus that consisted of two microscopes was developed for this task, as shown in Fig. 12. The two microscopes were perpendicular to each other to capture images in both the horizontal and vertical directions. Two types of glass spheres with 50-µm and 10-µm diameters were placed on the view-scopes of the microscopes and resin was applied to bond them to the stylus. The total bonding process usually lasted a relatively long time since the resin required 1 h to harden in a 140°C oven. Photographs of the finalized styli with new 50-µm and 10-µm sphere tips are shown in Fig. 13(a) and (b), respectively. After bonding, the adhesive forces between the glass spheres and the styli were evaluated using the same experimental setup described in the previous section. The 50-µm sphere had an adhesive force of 40 mN and the 10-µm sphere had an adhesive force of 2 mN. According to the contact force limitation described in Section 3.2, the 10-µm sphere cannot be used with this displacement probe.

3.6 Measurement of a micro-aspheric surface profile

Micro-aspheric surface profiles were measured using the contact-mode displacement sensor with a 50-µm sphere probe. The displacement probe was mounted on the air-bearing linear stage. A carbide micro-aspheric profile based on a brass substrate was vacuum-chucked on an air-spindle, as shown in Fig. 14. The stability of the displacement sensor on the linear stage was evaluated in advance while the probe shaft was pressed against the aspheric workpiece. The output of the displacement sensor, shown in Fig. 15, vibrated with an amplitude of 20 nm. We suspect that this vibration
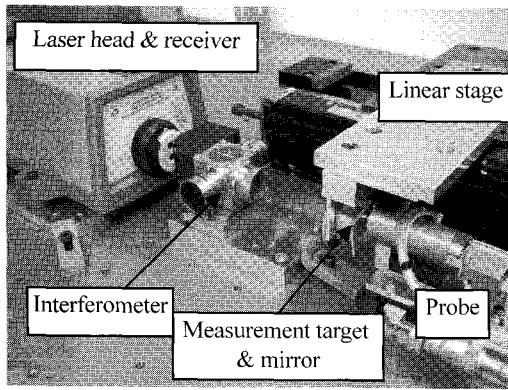
Fig. 8 Experimental setup used to evaluate the linearity of the displacement sensor
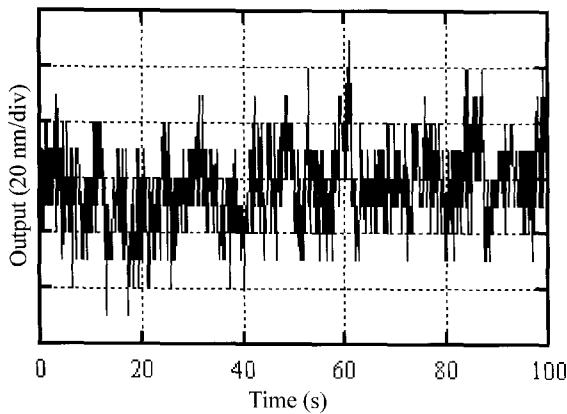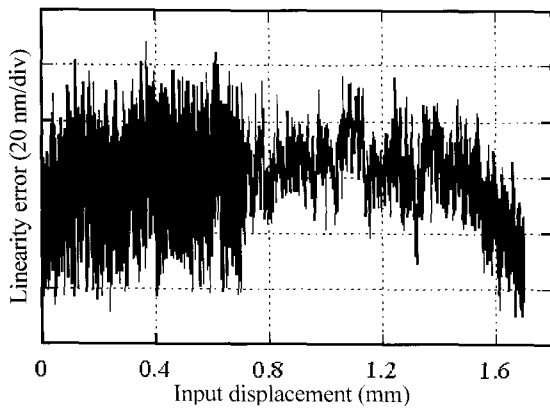

Fig. 9 Stability of the interferometer

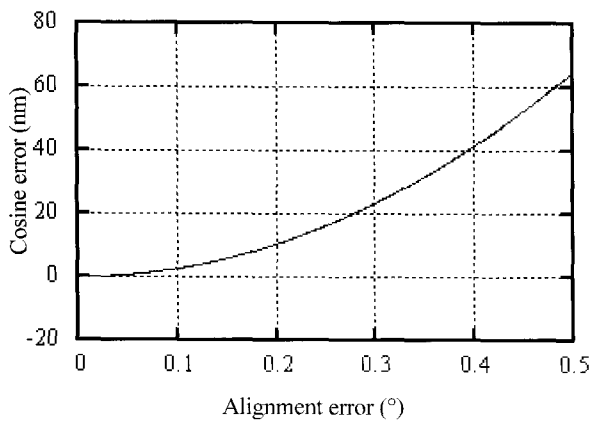Fig. 10 Linearity of the displacement sensor

Fig. 11 Effect of the alignment error

came from the linear stage since 20 nm peaks cannot be found in the stability evaluation in Section 3.1. During the micro-aspheric surface profile measurements, the output signal of the displacement sensor originated from the signal of the linear encoder, and the motion of the linear stage was set as a reference. The output of the displacement sensor was acquired and transferred to a PC through a counter board. The experimental conditions are given in Table 6 and the measured profile is shown in Fig. 16, where the horizontal axis presents the position of the linear stage, the left vertical axis gives the output of the displacement probe, and the right vertical axis indicates the reproducibility of two measurement procedures. The reproducibility was better than ±50 nm during the entire time that measurements were taken.
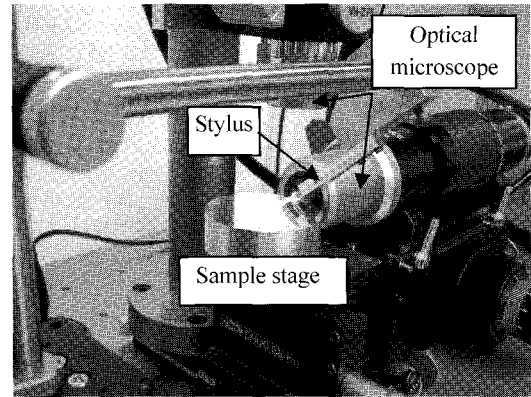

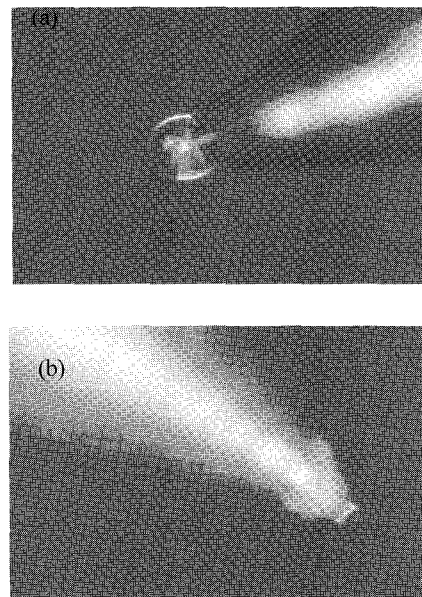Fig. 12 Experimental setup for bonding the microprobe sphere

Fig. 13 (a) Microscopic image of the 50-μm probe sphere
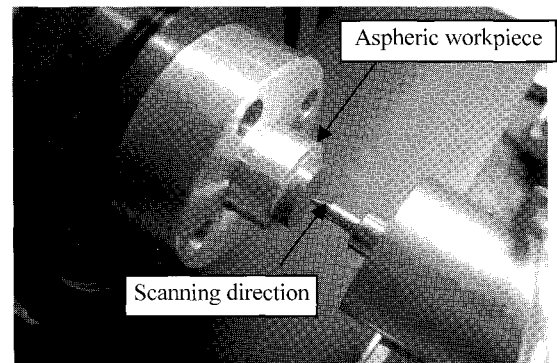(b) Microscopic image of the 10-μm probe sphere

Fig. 14 Photograph of the micro-aspheric profile measurements

Table 6 Experimental conditions used during the micro-aspheric profile measurements

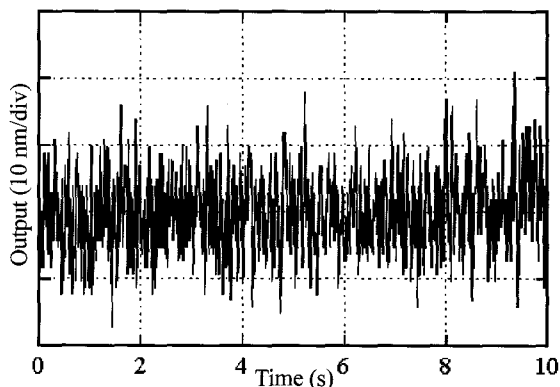| Scan length	1.5 mm
Sampling interval	4.4 μm
Sampling number	270
Measurement time	7.5 s

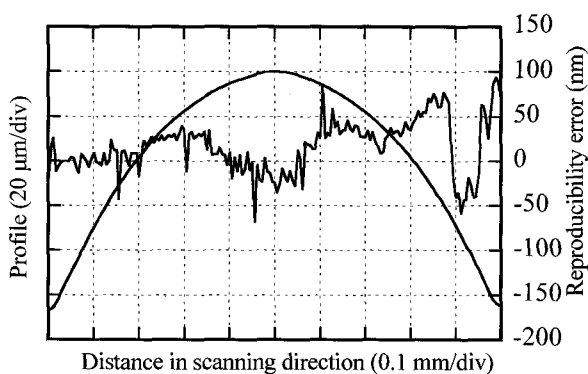Fig. 15 Stability of the contact-mode displacement sensor

Fig. 16 Micro-aspheric workpiece measurements

4. Discussion

Several issues exist regarding the new contact-mode displacement sensor that must be addressed.

The first is the 20-nm-amplitude vibration in the output of the displacement sensor. This likely arose from the vibration between the linear stage and the aspheric workpiece.

Second, we have to consider the effect of the motion errors of the system, which include the straightness error of the linear stage and the axial motion error of the spindle. These errors should be removed from the output of the displacement sensor.[6,7] In addition, since an aspheric profile usually has a large tilt angle, a tiny positioning error during its rotation on the spiral scanning system may cause a considerable measurement error in the final results.[8] The positioning errors of the linear stage along its direction of motion are usually more evident because the tilt angle can be larger in that direction. Figure 17 illustrates how the positioning errors affect the output of the displacement sensor, and Fig. 18 shows the motion and positioning errors that we must consider when using the spiral scanning method. Table 7 gives the values of each error, which combine to yield a final measurement error of ±10 nm for the measured micro-aspheric surface profile. The maximum tilt angle of the micro-aspheric workpiece was set to 60°.

Finally, the contacts point of the sphere–probe changes significantly when the sample is an aspheric surface with a tilt angle. This also introduces considerable errors to the output of the displacement probe. Consequently, the profile error of the sphere–probe must be calibrated in advance.[9]
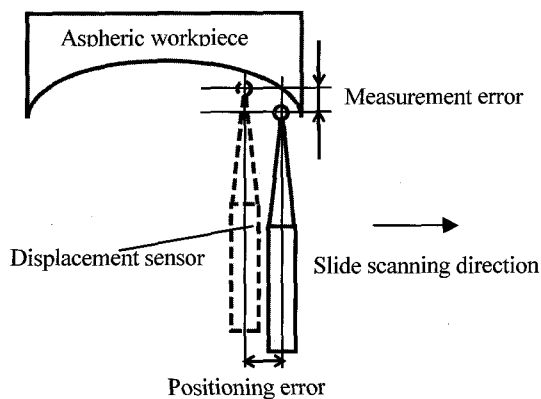

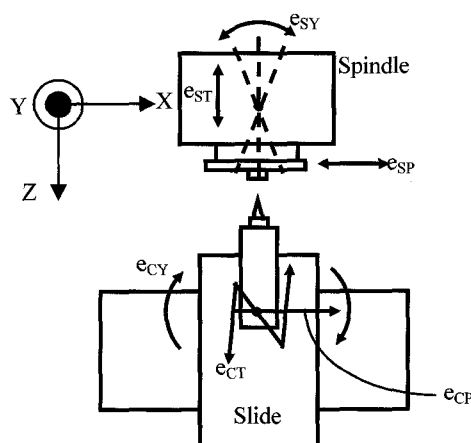Fig. 17 Effect of the positioning error on the measurement error

Fig. 18 Motion errors of the measurement system

Table 7 Motion errors corresponding to a ±10 nm measurement error

	Motion error	Amount
Slide	Horizontal straightness	±10 nm
	X-positioning	±6 nm
	Yawing	±75 nrad.
Spindle	Axial motion	±10 nm
	Radial motion (along the X-axis)	±6 nm
	Tilt motion (around the Y-axis)	±75 nrad.

5. Conclusions

A novel contact-mode scanning probe measuring system was developed for precise profile measurements of micro-aspheric surfaces. The new system has the capability of measuring micro-aspheric surfaces with large tilt angles and complex profiles. An air bearing was used to suspend the shaft of the probe to reduce the contact force, enabling fine adjustments of the contact force by changing the air pressure. The movement of the shaft was measured by a linear encoder with a scale that was attached to the actual shaft to avoid Abbe errors. A glass sphere with a 50-μm diameter was bonded to the tip of the air-bearing stylus to improve the lateral resolution of the system, providing a resolution as high as 10 nm. Several primary experiments were conducted that demonstrated the performance of the new measuring system.

ACKNOWLEDGEMENT

Energy and Industrial Technology Development Organization (NEDO).

REFERENCES

1. Seibel, E. J., Fauver, M., Crossman-Bosworth, J., Smithwick, Q. Y. J. and Brown, C. M., "Microfabricated optical fiber with microlens that produces large field of-view, video rate, optical beam scanning for microendoscopy applications," Proc. of the SPIE, Vol. 4957, pp. 46–55, 2003.

2. Yoshizumi, K., Murao, T., Masui, J., Imanaka, R. and Okino, Y., "Ultrahigh accuracy 3-D profilometer," Applied Optics, Vol. 26, No. 9, pp. 1647–1653, 1987.

3. Lee, C. O., Park, K., Park, B. C. and Lee, Y. W., "An algorithm for stylus instruments to measure aspheric surfaces," Measurement Science and Technology, Vol. 16, No. 5, pp. 1215–1222, 2005.

4. Teimel, A. and Heidenhahn, J., "Technology and applications of grating interferometers in high-precision interferometers in high-precision measurement," Precision Engineering, Vol. 14, No. 3, pp. 147–154, 1992.

5. Pantzer, D., Politch, J. and Ek, L., "Heterodyne profiling instrument for the angstrom region," Applied Optics, Vol. 25, No. 22, pp. 4168–4172, 1986.

6. Gao, W., Arai, Y., Shibuya, A., Kiyono, S. and Park, C. H., "Measurement of multi-degree-of-freedom error motions of a precision linear air-bearing stage," Precision Engineering, Vol. 30, No. 3, pp. 96–103, 2006.

7. Gao, W., Huang, P. S., Yamada, T. and Kiyono, S., "A compact and sensitive two-dimensional angle probe for flatness measurement of large silicon wafers," Precision Engineering, Vol. 26, No. 4, pp. 396–404, 2002.

8. Arai, Y., Gao, W., Shimizu, H., Kiyono, S. and Kuriyagawa, T., "On-machine measurement of aspherical surface profile," Nanotechnology and Precision Engineering, Vol. 3, No. 2, pp. 210–216, 2004.

9. Shibuya, A., Arai, Y., Gao, W. and Kiyono, S., "Testing of a probe for profile measurement of aspherical surface," Proc. 3rd Int. Conf. on Leading Edge Manufacturing in the 21st Century, pp. 331–334, 2005.